Photochemical Reactivity of $Sr_2Nb_2O_7$ and $Sr_2Ta_2O_7$ as a Function of Surface Orientation

Jennifer L. Giocondi, Ariana M. Zimbouski, and Gregory S. Rohrer
Department of Materials Science and Engineering, Carnegie Mellon University,
Pittsburgh, PA 15213-3890, U.S.A.

ABSTRACT

$Sr_2Nb_2O_7$ and $Sr_2Ta_2O_7$ have a (110) layered perovskite structure and are efficient photolysis catalysts. Aqueous silver and lead cations were photochemically reduced and oxidized, respectively, on the surfaces of $Sr_2Nb_2O_7$ and $Sr_2Ta_2O_7$ crystals with a wide range of orientations. Atomic force microscopy has been used to observe the distribution of photochemically reduced and oxidized products and determine the orientation dependence of the reactivity. On surfaces with the same orientation, reaction products frequently had a non-uniform distribution. The reactivity of both compounds proved to be only weakly anisotropic, with the highest relative reactivity for both oxidation and reduction occurring for surfaces oriented between (010), (110), and (011). These low index orientations have structures similar to the ideal {110} and {100} planes in the perovskite structure, respectively. The relationship of the perovskite structure to the reactivity is discussed.

INTRODUCTION

When illuminated with ultraviolet light, some ceramic oxides can dissociate water to form H_2 and O_2. In principle, it is therefore possible to directly convert solar energy to a clean burning, replenishable fuel. Systems based on particulate catalysts have attracted attention because of their potential to produce H_2 in relatively simple and inexpensive reactors. Such systems typically have low efficiencies because many of the photogenerated carriers recombine before reacting at the surface and much of the photochemically generated H_2 and O_2 undergoes a reverse reaction to form water before it can be separated. Therefore, significant amounts of water can be dissociated only if carrier recombination and the back reaction can be suppressed. For this reason, recent work has been directed toward the development of catalyst structures that separate the charge carriers and the H_2 and O_2 production sites [1].

Recently, a number of ternary transition metal oxide catalysts have been discovered to dissociate water more efficiently than conventional materials such as titania. These new materials all have anisotropic structures made up of layers [2,3] or tunnels [4,5]. It has been hypothesized that these materials have high efficiencies because the layers and tunnels somehow separate the photogenerated charge carriers and, therefore, the locations of the oxidation and reduction half reactions. If such a separation were to occur, it would suppress carrier recombination and the rate of the back reaction. Two such materials are $Sr_2Ta_2O_7$ (Cmcm, a = 3.937 Å, b = 27.198 Å, c = 5.692 Å) [6] and $Sr_2Nb_2O_7$ ($Cmc2_1$, a = 3.933 Å, b = 26.726 Å, c = 5.683 Å) [7]. Both of the structures are made up of corner sharing MO_6 octahedra that are arranged in (110) perovskite type slabs parallel to (010), and separated by Sr_2O layers. As Fig. 1 shows, the main difference between these materials is the distortion of the NbO_6 octahedra in $Sr_2Nb_2O_7$ which makes it ferroelectric (Ps || c-axis). The role that the layer structure plays in the superior photochemical properties of these compounds is currently unclear. [2,8].

The objective of the research described in this paper was to test the hypothesis that the

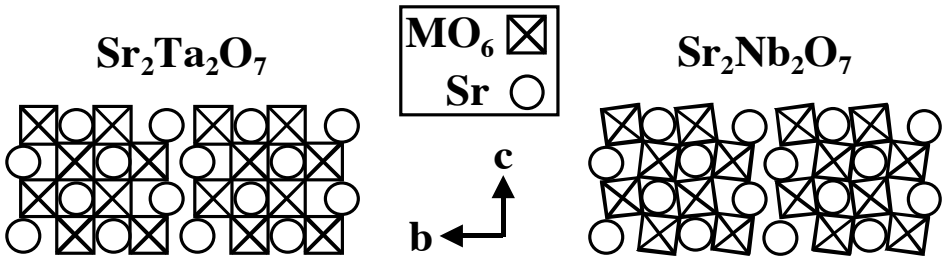

Figure 1. Schematic drawing of the layered perovskite structures of $Sr_2Ta_2O_7$ (Cmcm) and $Sr_2Nb_2O_7$ ($Cmc2_1$) parallel to [100].

photochemical reactivity of these layered materials is anisotropic. To test this idea, photochemical probe reactions that leave solid products at the reaction site have been carried out on surfaces with a wide range of orientations. The reduced silver and oxidized lead left behind by these reactions can be detected by standard microscopic techniques [9-12]. The amounts of the reaction products found on the different surfaces are taken as relative measures of a surface's reactivity [13]. If the reduced and oxidized products were found primarily on different surfaces, it would allow the important structural components for the oxidation and reduction reaction to be identified.

EXPERIMENTAL DETAILS

Polycrystalline $Sr_2M_2O_7$ ceramics were made by first reacting commercially available $SrCO_3$ (Alfa Aesar, 99%) and M_2O_5 (Ta_2O_5, Cerac, 99.5%; Nb_2O_5, Alfa Aesar, 99.5%) powders at 1400 °C for 100 h. Once X-ray diffraction confirmed that the powder was phase pure, the $Sr_2M_2O_7$ powder was uniaxially compacted under 150 MPa to form disk-shaped pellets with a thickness of 4 mm and an approximate diameter of 11 mm. The pellets were then placed in an alumina crucible with an excess of the parent powder to insure that the pellet did not contact the crucible. The samples were then processed in air to sinter the ceramics and grow the grains. The prepared ceramics were then lapped flat using a 3 μm Al_2O_3 (Buehler) aqueous solution and polished with a basic 0.02 μm colloidal silica solution (Buehler). Polished samples were annealed in air at 1200 °C to remove polishing damage, facet the surface, and thermally etch the grain boundaries.

Some surfaces were promoted with NiO before the photochemical reaction in the following way. A bare polycrystal as placed on a hotplate at approximately 150°C. A 0.05 M $Ni(NO_3)_{2\ (aq)}$ solution was sprayed on the surface until the coverage appeared macroscopically even. The sample was heated to 400 °C to calcine. It was then pretreated by reduction at 500°C for 1 h in forming gas (10% H_2/ 90% N_2) and reoxidation at 200°C for 1 h in O_2.

The photochemical reactions were carried out on the $Sr_2M_2O_7$ samples in the following way. A viton O-ring, 1.7 mm thick, was placed on the sample surface and the interior volume was filled with a solution containing either a 0.115 M aqueous $AgNO_3$ (Fisher Scientific) or a 0.0115 M aqueous $Pb(C_2H_3O_2)_2$ (Fisher Scientific) depending on the reaction to be studied. A 0.2 mm thick quartz cover slip was then placed on top of the O-ring and held in place by the surface tension of the solution. The sample was illuminated using a variable power, high pressure Hg lamp (300 W for silver reduction, 400 W for lead oxidation) for a fixed amount of time. After exposure, the sample was rinsed with deionized H_2O and dried with forced air. In control experiments conducted with light made up of energies less than either $Sr_2M_2O_7$'s band gap, no photochemical reactions were observed.

Atomic Force Microscopy (AFM) (Thermomicroscopes M5) was used to examine the surface topography both before and after the lead probe reaction. In this way, reaction sites, indicated by the presence of a solid product, could be directly correlated to preexisting surface features. Images of bare surfaces were acquired in contact mode while the images following a reaction were acquired using non-contact mode. All topographs presented in this paper are displayed in grayscale; light contrast indicates relatively high regions of the surface while dark contrast indicates relatively low areas of the surface.

After the AFM imaging was completed, the crystallographic orientations of individual grains in the polycrystalline samples were determined from electron backscattered diffraction patterns (EBSP). The samples were imaged in a Phillips XL40FEG scanning electron microscope. An EBSP was collected for each grain and the patterns were indexed using OIM for Windows Software, Ver.3 (TexSEM Laboratories, Inc.). The software returns a set of Euler angles (ϕ_1, Φ, ϕ_2) for each grain which are used to specify a relationship between the sample reference frame and the crystallographic axes. From these data, the components of the surface normals can be computed. Because some crystal orientations facet during the 1200 °C anneal, the surface normals computed from the EBSPs do not necessarily correlate to the crystallographic planes that bound the surface.

RESULTS

Figure 2 shows the results from the silver reduction reaction on $Sr_2Ta_2O_7$. This reaction was carried out with a 45 s exposure. A NC-AFM topograph of a typical area after the reaction is shown in Fig. 2a. The circular white contrast corresponds to silver deposits. The first feature to note is that the majority of the grains in this area are faceted. In fact, approximately 80% of the grains examined in this study have faceted surfaces. Therefore, in most cases, the planes that bound the surface are actually inclined with respect to the macroscopic surface normal.

It is also obvious from Fig. 2a that the silver islands are not deposited uniformly within the individual grains. The grain marked "X" in Fig. 2a is probably the best example of this phenomenon. There are silver deposits concentrated on the left hand side of this grain while the remainder of the grain has relatively few silver deposits. Also notice how silver deposits have accumulated in the grain boundary grooves as indicated by the white arrows. Although this deposition does not occur at all grain boundaries, it is frequently observed. Overall, the observed differences in the amounts of reaction products found on different grains are not as large as observed in previous studies of TiO_2 [13]. In the earlier studies, some grains were completely covered with reaction products while others were nearly free of products. By comparison, this reaction exhibits little anisotropy.

The activity of individual crystallites was estimated by counting the number of silver deposits on a representative area of each grain. In cases where the silver coverage was inhomogeneous, two representative areas were counted and averaged. The silver islands that deposited in the grain boundary grooves were not counted. Figure 2b is a plot of the activity of each grain examined as a function of the surface orientation. All grains were placed into one of three categories: low (0 - 3 deposits/μm), medium (3 – 6 deposits/μm), or high (6 - 23 deposits/μm). Grains with high activity typically had an even, dense, homogeneous coverage of silver. Low activity grains usually had a few deposits that were evenly spread across the surface. Most grains with an inhomogeneous silver coverage fell into the medium category. The grains that were most reactive are closer to (010) than the three other low index directions. In fact, most of

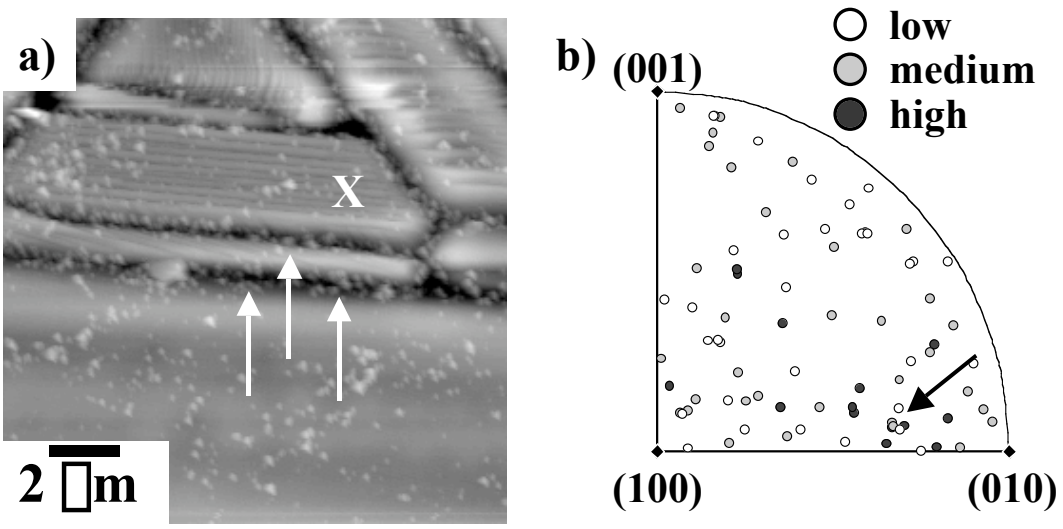

Figure 2. Photochemical activity results for a $Sr_2Ta_2O_7$ polycrystal after illumination in a silver nitrate solution. (a) NC-AFM topograph of a typical area. The areas of white contrast correspond to Ag^0 deposits. The white arrows indicate Ag^0 deposits accumulated in grain boundaries. "X" denotes a grain with inhomogeneous amount of Ag^0. The vertical black-to-white contrast is 50 nm. (b) Orientation-activity relationship for $Sr_2Ta_2O_7$ surfaces plotted on the standard stereographic triangle for orthorhombic crystals. The arrow indicates a group of grains with nearly the same orientation but different activities.

these grains lie between (010), (110), and (011). Indexed in terms of the ideal perovskite structure, the $Sr_2Ta_2O_7$(010) plane is structurally analogous to (110) and the $Sr_2Ta_2O_7$(110) and (011) planes are similar to (100). It should also be noted that there are several incidences of grains with nearly the same orientation that have very different activities (see arrow in Fig. 2b). The number of examples of these inconsistencies is larger than expected from experimental error and presumably arises from the inhomogeneous distribution of reaction products.

Like $Sr_2Ta_2O_7$, most of the $Sr_2Nb_2O_7$ grains are faceted. The results of the lead oxidation experiment on $Sr_2Nb_2O_7$ were similar to the silver reduction on $Sr_2Ta_2O_7$. The accumulation of oxidized lead was frequently inhomogeneous within a single grain and when the amounts of oxidized lead are plotted as a function of orientation, all of the grains with high activity have surface orientations between (010), (110) and (011).

It has previously been reported that it is necessary to use a NiO promoter with $Sr_2Nb_2O_7$ to observe any activity for water photolysis [3,8] and in our experiments, we find that the promoter is also required for the silver reduction reaction. Figure 3a is a topograph of the surface of a NiO-promoted polycrystal. The white contrast in this image corresponds to NiO (see arrows).

The silver reduction was then performed with a 15 s exposure. The NC-AFM image in Fig. 3b is of the surface in Fig. 3a after the silver reduction reaction. New areas of light contrast correspond to Ag deposits. Notice that the grain marked "X" in Figs. 3a and 3b had no noticeable NiO on the surface yet, it still had silver deposits after the reaction. We found that grains with high coverage of NiO did not necessarily have the highest amounts of silver. Experiments on the promoted surfaces were complicated by the fact that granular NiO and Ag are indistinguishable in AFM images. The amounts of silver were estimated from the most reliable images when the before and after images were easily compared and large differences could be measured. Based

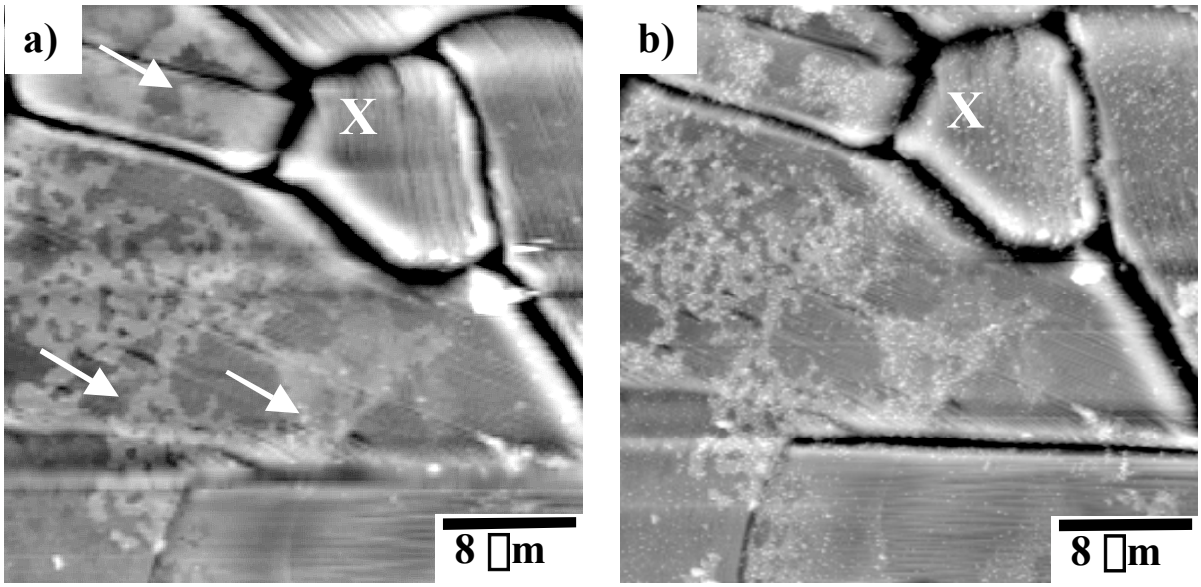

Figure 3. NC-AFM topographs the $Sr_2Nb_2O_7$ crystallites for both oxidation and reduction. (a) Area on a polycrystalline sample following the addition of a NiO promoter and the associated pretreatment. The areas of white contrast correspond to NiO deposits (see arrows). (b) The same area as in (a) following the reduction of silver. The new areas of white contrast correspond to Ag^0 deposits. Grain "X" appears to have no NiO in (a) but has silver deposits in (b). The vertical black-to-white contrast in (a) and (b) are 500 nm, and 500 nm, respectively.

on this analysis, we again find that the highest reactivity surfaces have orientations between (010), (110) and (011).

DISCUSSION

The results illustrate that both the oxidation and reduction reactions are favored on surfaces with orientations between (010), (110), and (011). In other words, within the resolution of our experiment, the oxidation and reduction reactions occur predominantly on the same crystallographic planes. The differences in the reactivities of different orientations were on the order of differences in the reactivity within single grains. The significant anisotropies previously observed in TiO_2 [13] and $SrTiO_3$ [14] are not detected here. The more isotropic reactivity of these layered compounds was not expected.

It is interesting to consider the current results in comparison to recent observations of the orientation dependence of the reactivity of a compound with the ideal perovskite structure, $SrTiO_3$ [14]. In this case, surfaces vicinal to (100) had the highest reactivity for silver reduction. In the $Sr_2Nb_2O_7$ and $Sr_2Ta_2O_7$ structures, the (110) and (011) planes have a configuration that is analogous to the structure of $SrTiO_3$(100). In the current experiment, the highest reactivity grains had orientations in the region between (010), (110) and (011). Since most of the grains were faceted, the macroscopic, average crystal orientations determined by EBSP were not identical to those of the planes terminating the surface. Since the (100) surface is known to be a low energy plane in perovskites, it is likely that facets on the surfaces of $Sr_2Nb_2O_7$ and $Sr_2Ta_2O_7$ had the analogous (110) and (011) orientations. Therefore, the relatively high reactivity of the (110) and (011) surfaces of $Sr_2Nb_2O_7$ and $Sr_2Ta_2O_7$ might be explained by the similarity of the

local configuration of atoms to the perovskite(100) surface. Additional tests on other transition metal oxide compounds with the perovskite structure would be required to support or refute this apparent structure-property relationship.

In the case of ferroelectric $Sr_2Nb_2O_7$, it has also been proposed that internal fields help separate the photogenerated charges [8]. This hypothesis is reasonable since previous studies on $BaTiO_3$ have shown that the dipolar fields associated with the ferroelectric domains do, in fact, separate the charges and, therefore, the oxidation and reduction half reactions [15]. If dipolar fields are the important charge separation mechanism for $Sr_2Nb_2O_7$, then we would expect to find grains with high reactivity oriented perpendicular to the direction of the spontaneous polarization, [001]. The few grains we observed with this orientation had relatively low reactivity and showed no evidence for the domain patterns observed in studies of $BaTiO_3$ [15]. Future studies will concentrate on more detailed studies of grains with this particular orientation.

CONCLUSIONS

The photochemical reduction of Ag and oxidation of Pb on $Sr_2Nb_2O_7$ and $Sr_2Ta_2O_7$ occurs most readily on surfaces oriented between (010), (110), and (011). The (110) and (011) surfaces are structurally similar to perovskite(100), which is the most reactive of $SrTiO_3$ surfaces.

ACKNOWLEDGEMENTS

This work was supported primarily by the National Science Foundation under grant number DMR-0072151. The work was supported in part by the MRSEC program of the National Science Foundation under award number DMR-0079996, though use of shared experimental facilities.

REFERENCES

[1] K. Domen, in *Surface Photochemistry,* edited by M. Anpo (J. Wiley and Sons, Chichester, England, 1996) p. 1.
[2] D.W. Hwang, H.G. Kim, J. Kim, K.Y. Cha, Y.G. Kim, and J.S. Lee, J. Catalysis **193**, 40 (2000).
[3] T. Takata, Y. Furumi, K. Shinohara, A. Tanaka, M. Hara, J.N. Kondo, and K. Domen, Chem. Mat. **9**, 1063 (1997).
[4] M. Kohno, S. Ogura, K. Sato, and Y. Inoue, J. Chem. Soc., Faraday Trans. **94** (1), 89 (1998).
[5] Y. Inoue, T. Kubokawa, and K. Sato, J. Phys. Chem. **95**, 4059 (1991).
[6] N. Ishizawa, F. Murumo, T. Kawamura, and M. Kimura, Acta Crystallogr. **B32**, 2464 (1976).
[7] N. Ishizawa, F. Murumo, T. Kawamura, and M. Kimura, Acta Crystallogr. **B31**, 1912 (1975).
[8] A. Kudo, H. Kato, and S. Nakagawa, J. Phys. Chem. B **104**, 571 (2000).
[9] J.-M. Herrmann, J. Disdier, and P. Pichat, J. Catalysis **113** (1), 72 (1988).
[10] W.C. Clark and A.G. Vondjidis, J. Catalysis **4** (6), 691 (1965).
[11] K. Tanaka, K. Harada, and S. Murata, Solar Energy **36**, 159 (1986).
[12] J. Torres and S. Cervera-March, Chem. Eng. Sci. **47**, 3857 (1992).
[13] J.B. Lowekamp, G.S. Rohrer, P.A. Morris Hotsenpiller, J.D. Bolt, and W.D. Farneth, J. Phys. Chem. B **102** (38), 7323 (1998).
[14] J.L. Giocondi and G.S. Rohrer, J. Amer. Ceram. Soc., submitted.
[15] J.L. Giocondi and G.S. Rohrer, Chem. Mater. **13** (2), 241 (2001).